Radboud university

Bachelor thesis

Department: Theory of condensed matter

Computing the Hopf index for a magnetic lattice

Author: Rens Theunissen
Supervisor: Dr. Misha Titov
Second supervisor: Dr. Uli Zeitler

November 5, 2021

Abstract

This thesis's main topic is about finding new energy models which could house a hopfion. In order to achieve this many computer simulations need to be run. They are performed using python and uses the SPIRIT module[1]. All of these simulations are checked to see if a hopfion has formed, to do this the Hopf index is used. This paper gives an outlook on things to improve in simulations for future research and a basic way to perform Hopf index calculations.

Acknowledgements

I would like to thank Dr. Titov for supervising me during this thesis even when the Covid-19 pandemic was going on, and enabling me to perform some research at the Theory of condensed matter department. I'd also like to thank him for helping me with figuring out the calculations in this thesis.

Contents

1 Introduction

As technology has been further developed and improved in the last decades, the need for better, more complex materials has grown with it. This demand leads to a need to understand the properties of materials and how to manipulate said properties properly which makes it an important research topic in condensed matter theory. One of these material properties is the appearance of topological solitons, which are topological particles/quasi-particle which propagate as non-dissipative waves.

A hopfion, a 3D quasi-particle, is one of such topological solitons and a fairly new topic of interest which is justified by their easy to understand motion induced by electrical current even though they have a non-trivial topology. Even though hopfions have been theoretically proven to exist in the nano-meter size range, they have yet to be found. To make sure these nano-meter sized hopfions are found in the near future, it is important to have a lot of energy models that house hopfions available to be experimentally tested. The goal of this thesis is to find new energy models which could house hopfions by running many simulations using the SPIRIT module[1], these simulations will perform energy minimisation's on a micro magnetic system in the hopes that some result in a hopfion configuration. To make sure these simulations have some chance of succeeding the basis for the energy model will be the Heisenberg Hamiltonian.

This thesis is divided in 5 main chapters. Firstly, the theoretical background of hopfions themselves, the basis for the energy model and the background to the Hopf index will be given in section 2. In section 3 the method of running the simulation and the way how to calculate the Hopf index will be described. Section 4 will contain the results of the simulations. The conclusion is in section 5 and section 6 contains the discussion on how to improve the research.

2 Theory

2.1 Hopfions

2.1.1 Overview

Hopfions, also known as Faddeev-Hopf knots, are a type of three dimensional smooth quasi-particle known as a topological soliton. Hopfions appear in classical field theories and are stable, have a finite mass and were proposed by Ludvig D. Faddeev [2] as a limit solution to the Skyrme model. The Skyrme model describes composite 2-quark particles, also known as hadronic, physics [3]. In recent years hopfions are becoming a topic of interest in condensed matter theory as they could appear in the magnetisation or polarisation fields of certain materials. Unfortunately, due to the fact that hopfions are typically described by non-linear partial differential equations they cannot appear in most condensed matter systems as stated in the Hobart-Derrick theorem [4]. This theorem proves that there can't exist stable, three dimensional solutions for non-linear equations, which is exactly what a hopfion is. The Hobart-Derrick theorem also postulates how to avoid its statement, one of the ways to do so is by breaking the spatial inversion symmetry of material; this is the case for certain magnetic materials[5]. Hopfions have a non-zero Hopf number and are classified by their Hopf index, which generally determines the shape of the isolines of the hopfions as seen in figure 1, these isolines combined with the angular parameter Φ describe the isosurface of said hopfion. The general shape of the isosurface is that of a knotted torus and the complexity of the knot is dependent on the isolines and thus can be linked to the Hopf index.

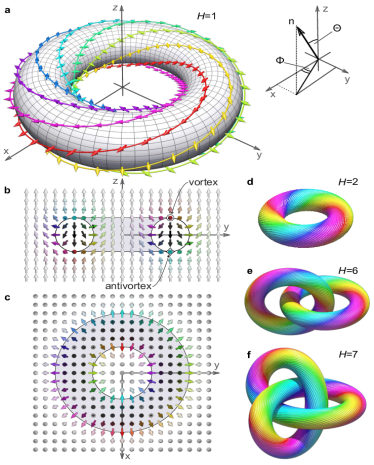

Figure 1: Typical structures of hopfions. a, Toroidal hopfion with Hopf index H = 1. The solid colored isolines connect points r of a vector field n(r) = (cos(Φ) sin(Θ), sin(Φ) sin(Θ), cos(Θ)) with fixed values of angular variables, $\Theta = \Theta(r)$ and $\Phi = \Phi(r)$. The color of the vectors and the corresponding isolines are defined by the angular parameter Φ and together they compose the isosurface Θ = const. b and c, Texture of toroidal hopfion at intersecting planes x = 0 and z = 0, respectively. d-f, Isosurfaces Θ = const for toroidal hopfion with H = 2, two linked toroidallike hopfions with total H = 6, and for hopfion with trefoil knot-like shape with H = 7 [6]

2.1.2 Hopfions outside of simulations

As more and more numerical models predict the existence of hopfions [7] the search for them in physical systems is getting increasingly important. Recently, micrometer sized magnetic hopfions were observed in a condensed matter system [8] but, the search for nano-meter sized hopfions hasn't succeeded yet. This will likely change in the near future as the amount of research going into this subject is increasing each year.

2.2 Hopfion Energy model

The general energy model used in this thesis is based on the extended Heisenberg Hamiltonian[1]:

$$\mathcal{H} = E_{Mag} + E_{Ex} + E_{DMI} + E_{Ani} \tag{1}$$

where E_{Mag} is the Zeeman energy term, E_{Ex} is the exchange energy term, E_{DMI} the Dzyaloshinskii-Moriya energy term and E_{Ani} is the magnetic anisotropy energy term:

$$E_{Mag} = -\sum_i \mathbf{B} \cdot \mathbf{m}_i \tag{2}$$

$$E_{Ex} = -\sum_{\langle ij \rangle} J_{ij} \mathbf{n}_i \cdot \mathbf{n}_j \tag{3}$$

$$E_{DMI} = -\sum_{\langle ij \rangle} \mathbf{D}_{ij} \cdot (\mathbf{n}_i \times \mathbf{n}_j) \tag{4}$$

$$E_{Ani} = -\sum_i \sum_j K_j (\hat{K_j} \cdot \mathbf{n}_i)^2 \tag{5}$$

where $\mathbf{B}$ the external magnetic field in units T, J_{ij} is the exchange constant between the sites i and j in units J/m, $\mathbf{D}_{ij}$ is the DMI strength between the sites i and j in units J/m^2 , n_i are classical spins of unit length, $\hat{K_j}$ the magneto-crystalline anisotropy direction and K_j is the anisotropy strength in units J/m^3, m_i is the magnetisation at site i in units A/m which is given by the formula[1]:

$$\mathbf{m}_i = \mu_i \mathbf{n}_i \tag{6}$$

The extended Heisenberg Hamiltonian can contain a dipole-dipole interaction term but, this term has been omitted as it is small in nano sized systems and it increases the computation time due to its long-ranged nature. Higher order perturbation terms to the exchange interaction such as the quadruplet interaction[1]

$$E_{quad} = \sum_{ijkl} K_{ijkl} (\mathbf{n}_i \cdot \mathbf{n}_j)(\mathbf{n}_k \cdot \mathbf{n}_l) \tag{7}$$

have also been omitted in this thesis as it is not necessary to include them in the simulations.

2.2.1 Exchange interaction

The exchange interaction follows from the Pauli exclusion principle which states that no two identical fermions can occupy the same quantum state. This statement is equivalent to the statement that the total wave-function of a fermionic system must be anti-symmetric with respect to exchange. A consequence of this is that such a wave-function has either a symmetric spatial part and a anti-symmetric spin part or vice versa. The energy of these configurations is not the same and the difference in energy between these configurations is called the exchange energy. For a two electron system the exchange interaction in the continuous limit is described by the following equation:

$$J_{ex} = \int \int \frac{\phi_i(\mathbf{r}_1)^* \phi_j(\mathbf{r}_2)^* \phi_j(\mathbf{r}_1) \phi_i(\mathbf{r}_2)}{r_{12}} d\mathbf{r}_1 d\mathbf{r}_2 \tag{8}$$

From the exchange energy, specifically the exchange constant J_{ij}, it can be determined if a system is ferromagnetic or anti-ferromagnetic by looking at the sign of the J_{ij}. For $J_{ij} < 0$ the energy of the system will be minimal for a ferromagnetic ordering ($\hat{m_i} = \hat{m_j}$) of the vectors. If $J_{ij} > 0$ the system prefers a anti-ferromagnetic configuration ($\hat{m_i} = -\hat{m_j}$).

2.2.2 Dzyaloshinskii-Moriya interaction

The Dzyaloshinskii-Moriya interaction, also known as the anti-symmetric exchange interaction, contributes to the total exchange interaction. Rewriting the expression from equation 4:

$$E_{DMI} = -\sum_{\langle ij \rangle} \mathbf{D}_{ij} \cdot (\mathbf{n}_i \times \mathbf{n}_j) = -\sum_{\langle ij \rangle} (\mathbf{D}_{ij} \cdot \hat{n}) \sin(\phi_{ij}) \tag{9}$$

where ϕ_{ij} is the angle between two spin spirals. It becomes clear that the DMI term prefers the canting of spins structures (as that is more energetically favourable), such as spin spirals, since equation 9 is maximal for $\phi = \pm\frac{\pi}{2}$. Two things are important for the occurrence of the DMI term, they are spin-orbit coupling and an inversion-asymmetric environment; such an environment can be created by introducing a surface.

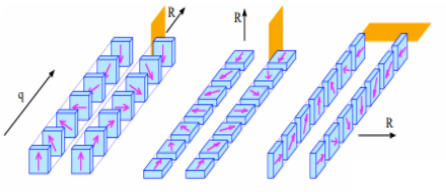

Figure 2: Flat spin spirals rotated around a rotation axis R which is pointing in different directions. When the initial spin spiral (left spiral of each pair) is mirrored on an appropriate mirror plane, the resulting spiral (right spiral of each pair) is the same as the initial one but, with a change of sign in q.[9]

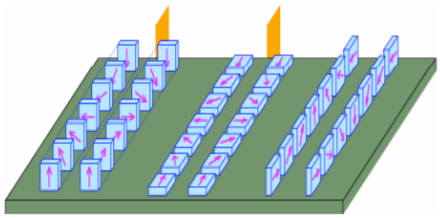

Figure 3: The same spin spirals as in figure 4.1 are shown again in this image, but now a surface is introduced under the spin spirals which breaks the symmetry of the environment.[9]

The direction and magnitude of the $\mathbf{D}_{ij}$ vector in a crystal is directly related to the symmetries of the neighbouring vectors: consider two points, one sited at $\mathbf{R}_1$ and the other sited at $\mathbf{R}_2$, the center of this two point system is then defined with a new vector $\mathbf{R}_3 = (\mathbf{R}_1 + \mathbf{R}_2)/2$. With these vectors the following relations are determined[10]:

- If a center of inversion is located at $\mathbf{R}_3$ then: $\mathbf{D}_{ij} = 0$
- If a mirror plane which is perpendicular to $\mathbf{R}_1\mathbf{R}_2$ passes through $\mathbf{R}_3$ then: $\mathbf{D} \parallel$ mirror plane or $\mathbf{D} \perp \mathbf{R}_1\mathbf{R}_2$
- If a mirror plane includes the positions $\mathbf{R}_1$ and $\mathbf{R}_1$ then: $\mathbf{D} \perp$ mirror plane
- If a two-fold rotation axis is perpendicular to $\mathbf{R}_1\mathbf{R}_2$ and passes through $\mathbf{R}_3$ then: $\mathbf{D} \perp$ two-fold rotation axis
- If there is an n-fold rotation axis with n ≥ 2 along $\mathbf{R}_1\mathbf{R}_2$ then: $\mathbf{D} \perp \mathbf{R}_1\mathbf{R}_2$

2.2.3 Magnetic-crystalline anisotropy

It is important to know how a systems magnetic properties depend on direction; if the properties are the same for all directions the system is called magnetically isotropic. If this isn't the case the system is called magnetically anisotropic. In an anisotropic material, some directions are energetically more favourable then others; these directions are called 'easy axis'. In this research a type of magneto-crystalline anisotropy is used. This anisotropy is mostly caused by spin-orbit interactions in a crystal. The easy axis for this type of anisotropy is dependent on the lattice type of the crystal as can be seen in figure 4.

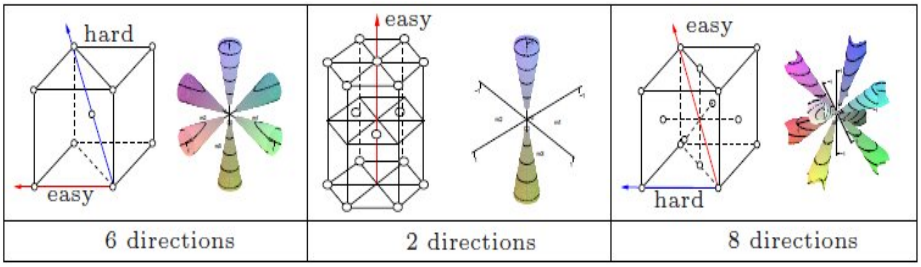

Figure 4: Easy and hard axis for a bcc, hexagonal and fcc lattice. [11]

2.2.4 Zeeman energy

The Zeeman energy, also known as the external field energy, is a type of potential energy that occurs when a magnetic material is located inside of a external magnetic field. In this field, the magnetisation vectors **m** of the magnetic material will shift to try to point in the same direction as the external magnetic field-lines point. **B**.

2.3 Hopf index

To understand the characteristics of the Hopf index, it is useful to look at its derivation and the Hopf invariant. The Hopf invariant, in the case of the continuous mapping from the unit three-sphere to the unit two-sphere

$$\mathbb{S}^3 \longmapsto \mathbb{S}^2 \tag{10}$$

is a homotopy invariant of said mapping[12]. Map 10 can be rewritten using the stereographic projection, which projects a sphere on a plane.

$$\mathbb{R}^3 \cup \infty \leftrightarrow \mathbb{S}^3 \tag{11}$$

$$\mathbb{R}^3 \cup \infty \longmapsto \mathbb{S}^2 \tag{12}$$

From these equations it becomes clear that continuous uniform three dimensional vector fields which are homogeneous at infinity can represent map 10.

These sorts of maps have a useful property, their set of homotopy classes is an isomorphism with integers.

$$\pi_3(\mathbb{S}^2) = \mathbb{Z} \tag{13}$$

This important expression states that, for a continuous unit vector field which is homogeneous at infinity, there exist an integer number called the Hopf index which won't change if the vector field is smoothly deformed. Additionally, vector fields which have the same Hopf index can be changed into each other by continuous deformation. All these characteristics make using the Hopf index incredibly useful as a way to classify hopfions.
The Hopf index can be calculated by using the linking numbers or, as done in this paper, by using the integral formula which is defined as [13]:

$$H = -\frac{1}{(8\pi)^2} \int \mathbf{F} \cdot \mathbf{A}\, d\mathbf{r} \tag{14}$$

wherein $\mathbf{F}$ can be seen as the gyrovector density[14] and $\mathbf{A}$ is the vector potential of $\mathbf{F}$. The components of $\mathbf{F}$ are defined as:

$$F_i = \epsilon_{ijk} \mathbf{n} \cdot (\partial_j \mathbf{n} \times \partial_k \mathbf{n}) \tag{15}$$

where $\mathbf{n}$ is a continuous smooth unit vector field. The relation between $\mathbf{F}$ and $\mathbf{A}$ is given by the following equation.

$$\mathbf{F} = \nabla \times \mathbf{A} \tag{16}$$

From equation 16 it can be seen that the vector field $\mathbf{A}$ has a gauge freedom. To be more precise, for a cubic lattice with N lattice point per direction the vector field $\mathbf{A}$ contains N^3 vectors of which N can be chosen freely.

3 Method

3.1 Simulation

The simulations are performed on Linux using a 10th generation intel i7 core processor, the code was written using the Python language using the Spirit library[1]. With the Spirit library, a system of magnetisation vectors is introduced by defining a lattice and energy function. The actual minimisation of the energy is performed by assigning a method and a solver to the system. For this research, the method will always be the Landau-Lifshitz-Gilbert equation and and the solver will always be the Verlet-like velocity projection solver[15].
The lattice is chosen to be a simple cubic lattice with periodic boundary conditions in all directions. To break the symmetry of the system, a one-atom sized vacancy is introduced in the lattice.

3.1.1 Energy function

As mentioned before, the simulations will use a Heisenberg Hamiltonian of the from given in formula 1. This Hamiltonian will always contain a Zeeman energy term given by equation 2, an exchange energy term given by equation 3 and, because energy functions describing hopfions are mostly non-linear, it will contain one or more non-linear term(s). These terms will be an anisotropic interaction of the form:

$$E_{Ani} = -K_b(1 - m_z^2) \tag{17}$$

and/or a DMI term of the form[16]:

$$E_{DMI} = D_b \mathbf{m} \cdot (\nabla \times \mathbf{m}) \tag{18}$$

where K_b and D_b are the bulk magnetic anisotropy and bulk DMI strength respectively.

3.2 Calculation of the Hopf index

To calculate the Hopf index some approximations need to be used. Firstly, it is important to rewrite formula 14 for a discrete lattice:

$$H = \frac{1}{(8\pi)^2} \sum_{\mathbf{r}} \mathbf{F}(\mathbf{r}) \cdot \mathbf{A}(\mathbf{r}) \tag{19}$$

where $\mathbf{r}$ is the position of a vector in the fields $\mathbf{F}$ and $\mathbf{A}$. For the calculation of all the vector components in the vector field $\mathbf{F}$ the derivatives of the magnetisation directions have to be computed. This is achieved by approximating them using the finite difference method, with these approximations equation 15 can be rewritten as:

$$F_l(l,m,n) \simeq \mathbf{n}(l,m,n) \cdot ((\mathbf{n}(l,m{+}1,n) - \mathbf{n}(l,m{-}1,n)) \times (\mathbf{n}(l,m,n{+}1) - \mathbf{n}(l,m,n{-}1)) \tag{20}$$

$$F_m(l,m,n) \simeq -\mathbf{n}(l,m,n)\cdot((\mathbf{n}(l{+}1,m,n){-}\mathbf{n}(l{-}1,m,n))\times(\mathbf{n}(l,m,n{+}1){-}\mathbf{n}(l,m,n{-}1)) \tag{21}$$

$$F_n(l,m,n) \simeq \mathbf{n}(l,m,n)\cdot((\mathbf{n}(l{+}1,m,n){-}\mathbf{n}(l{+}1,m,n))\times(\mathbf{n}(l,m{+}1,n){-}\mathbf{n}(l,m{-}1,n)) \tag{22}$$

after which all components of $\mathbf{F}$ can be calculated.
For the calculation of the vector field $\mathbf{A}$, it is import to choose a suitable gauge to fix the system. The gauge, in this case will, be the Coulomb gauge and is given below.

$$\nabla \cdot \mathbf{A} = 0 \tag{23}$$

Now take equation 16 and rewrite it as a double curl product:

$$\nabla \times \mathbf{F} = \nabla \times (\nabla \times \mathbf{A}) = \nabla(\nabla \cdot \mathbf{A}) - \nabla^2 \mathbf{A} \tag{24}$$

equation 24 can be simplified by applying the Coulomb gauge into:

$$\nabla \times \mathbf{F} = -\nabla^2 \mathbf{A} \tag{25}$$

which is a Poisson equation. Since the equation for the Hopf index assumes that the system is infinitely large the standard solution for the Poisson equation can be used as a valid approximation for $\mathbf{A}$. This equation is given by:

$$\mathbf{A}(\mathbf{r}) = \int_V \frac{(\nabla \times \mathbf{F})(\mathbf{r}')}{4\pi|\mathbf{r} - \mathbf{r}'|} d\mathbf{r}'^3 \tag{26}$$

rewriting this equations for a discrete system it becomes:

$$\mathbf{A}(\mathbf{r}) = \sum_{\mathbf{r}' \neq \mathbf{r}} \frac{(\nabla \times \mathbf{F})(\mathbf{r}')}{4\pi|\mathbf{r} - \mathbf{r}'|} \tag{27}$$

now the total equation for the Hopf index can be rewritten using equation 27:

$$H = \frac{1}{(8\pi)^2} \sum_{\mathbf{r}} \mathbf{F}(\mathbf{r}) \cdot \sum_{\mathbf{r}' \neq \mathbf{r}} \frac{(\nabla \times \mathbf{F})(\mathbf{r}')}{4\pi|\mathbf{r} - \mathbf{r}'|} \tag{28}$$

The accuracy of this Hopf index equation largely depends on the accuracy of the approximations. Because of the approximations, the Coulomb gauge isn't automatically satisfied, which also means that equation 16 isn't exact. This makes it important to check the calculation on some examples with an already known Hopf index. This is done by calculating the Hopf index, variance in the divergence of the vector field $\mathbf{F}$, variance in the coulomb gauge and variance in the equation $\mathbf{F} - \nabla \times \mathbf{A} = 0$ for the trivial system with all spins pointing in the same direction and for systems which already contain a hopfion of which the Hopf index is known.
The time it takes to perform the Hopf index calculation is highly dependent on the lattice size. This is because for every lattice site **r** the calculation has to sum over every other lattice site **r'** so the calculation time increases quite quickly.

4 Results

4.1 Hopf index

The code for the calculation of the Hopf index has been tested for accuracy on simple cubic lattices ranging in size from 9x9x9 atoms per direction to 23x23x23 atoms per direction for three situations (from now on the size of the lattices will be written as one number; so 23x23x23 will just be 23). In the first situation all spins point in the same direction, this field has a Hopf index of 0. In the second and third situation a hopfion is placed in the middle of the lattice, one of radius 2 and the other of radius 3; all vectors outside of the point in the same direction. The Hopf index of both these situations should be 1. For the same three systems the variance in the divergence of the field $\mathbf{F}$, the variance in the Coulomb gauge and the variance in the equation $\mathbf{F} - \nabla \times \mathbf{A} = 0$ is calculated. The calculated values for the Hopf index are in table 1 and the calculated values for the variances are in table 2, 3 and 4:

Lattice size	Situation 1	Situation 2	Situation 3
9	0	0.8805764066	1.2122805238
11	0	0.9656830426	1.5100991158
13	0	0.9917092126	1.7033530544
15	0	0.9936037994	1.8023184558
17	0	0.9936037994	1.8526712500
19	0	0.9936037994	1.8733942992
21	0	0.9936037994	1.8775157037
23	0	0.9936037994	1.8775157037

Table 1: Hopf index calculation for three different situations on different lattice sizes

lattice size	Situation 1 variance of $\nabla \cdot A$	Situation 2 variance of $\nabla \cdot A$	Situation 3 variance of $\nabla \cdot A$
9	0	1.6675765812	1.2730868587
11	0	1.3387931892	1.3285277682
13	0	1.0147982524	1.2515965646
15	0	0.8105337215	1.0431353853
17	0	0.6669142386	0.8417370812
19	0	0.5621288297	0.6957037846
21	0	0.4826429361	0.5937025618
23	0	0.4204887222	0.5148898974

Table 2: Variance in the Coulomb gauge for three different situations on multiple lattice sizes

lattice size	Situation 1 variance of $\mathbf{F} - \nabla \times \mathbf{A}$	Situation 2 variance of $\mathbf{F} - \nabla \times \mathbf{A}$	Situation 3 variance of $\mathbf{F} - \nabla \times \mathbf{A}$
9	0	2.6051047615	2.8465159064
11	0	2.0585129654	2.2346217001
13	0	1.5783402983	1.8615142283
15	0	1.2666624080	1.5604343150
17	0	1.0481062426	1.2884583616
19	0	0.8858919644	1.0730016802
21	0	0.7617388886	0.9170007021
23	0	0.6641984622	0.7985414745

Table 3: Variance in the difference between the vector field $\mathbf{F}$ and the vector field $\nabla \times \mathbf{A}$ for three different situations on multiple lattice sizes

lattice size	Situation 1 variance of $\mathbf{F}$	Situation 2 variance of $\mathbf{F}$	Situation 3 variance of $\mathbf{F}$
9	0	0.6129476556	0.7890844538
11	0	0.3194394115	0.4464258915
13	0	0.2072876928	0.2400568263
15	0	0.1635714969	0.1973521560
17	0	0.1355723533	0.1012577504
19	0	0.1147398071	0.0709826753
21	0	0.0987451047	0.0558891846
23	0	0.0861495003	0.0487601419

Table 4: Variance in the divergence of the vector field $\mathbf{F}$ for three different situations on multiple lattice sizes

By looking purely at the values in table 1, it becomes clear that for situation 2 and 3 the value of the Hopf index stabilises when the lattice reaches a critical size relative to the size of the hopfion contained in the lattice. This happens because at a certain lattice size the hopfion sits far away enough from the boundaries of the system such that the system size can be approximated as infinite. For situation 2, this critical size is 15x15x15 and for situation 3 it is 21x21x21.
The correlation between the calculation of the Hopf index and the variance of both the divergence and the equation $\mathbf{F} - \nabla \times \mathbf{A} = 0$ index depends on the situation. The correlation for situation 1 is 100% accurate, as can be seen from both variances for said situation in table 2, which is expected. All values for the variances of situation 1 are zero, because equation 15 contains derivatives which are automatically zero if all neighbouring vectors point in the same direction due to the approximation used. The correlation for situation 2 and 3 is more interesting; the variance for both situations keeps deceasing with increasing lattice size, whilst the Hopf index stabilises at a critical lattice size after which

it doesn't change anymore. This seems contradictory but, it is explained by situation 1. From situation 1, we can conclude that vectors that point in the same direction as their neighbouring vectors don't contribute to the Hopf index; this is why the Hopf index doesn't change past the critical lattice size even though we add more vectors pointing in the same direction. But, these vectors do contribute to the variance of the system. This contribution decreases the variance of both the divergences and of the equation $\mathbf{F} - \nabla \times \mathbf{A} = 0$.
This same correlation seems to also be in effect for the divergence of the vector field $\mathbf{F}$ as seen in table 4. The variance of the system in situation 2 and 3 keeps decreasing even though the Hopf index stops decreasing.
The actual accuracy of the value of the Hopf index seems to be varying. For situation 1 and 2 the calculation is quite accurate, but for situation 3 it is far off.

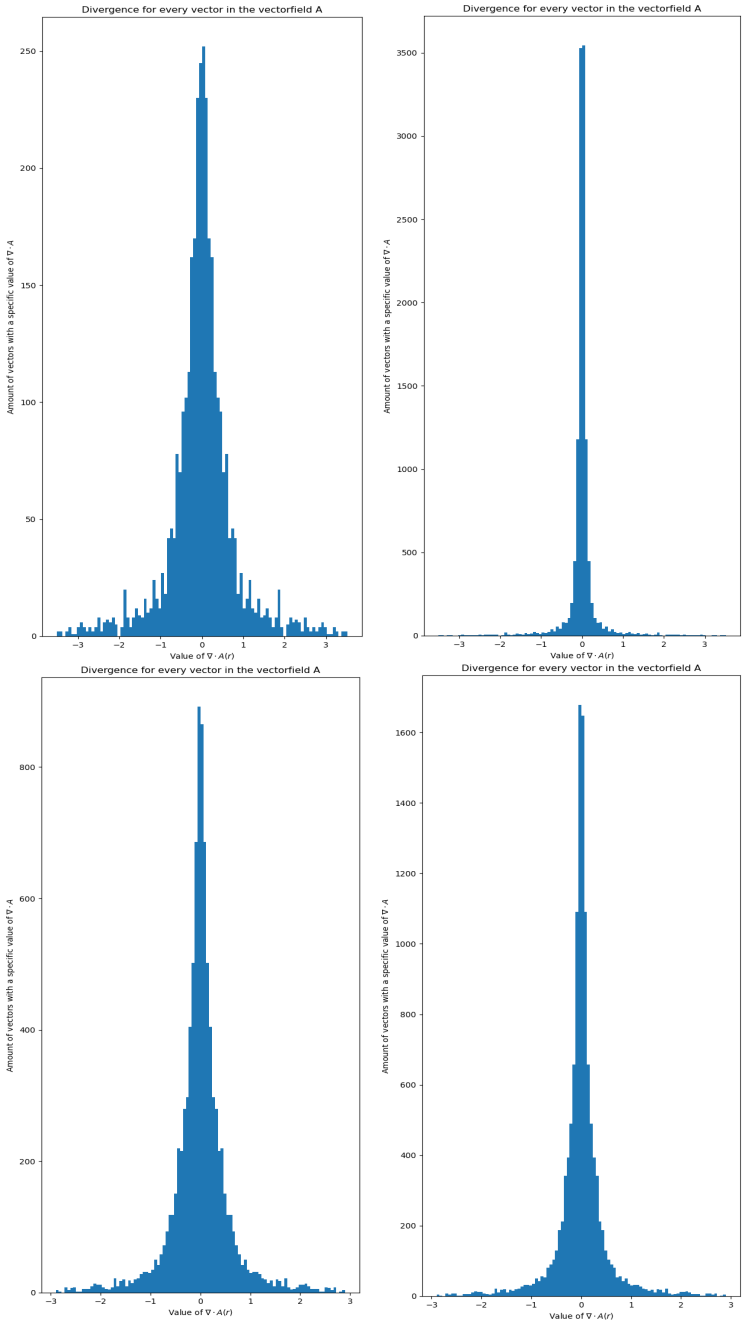

Figure 5: Divergence of every vector in the vector field **A** for different situations. Upper left: situation 2, lattice size 15x15x15. Upper right: situation 2, lattice size 23x23x23. Lower left: situation 3, lattice size 21x21x21. Lower Right: situation 3, lattice size 23x23x23

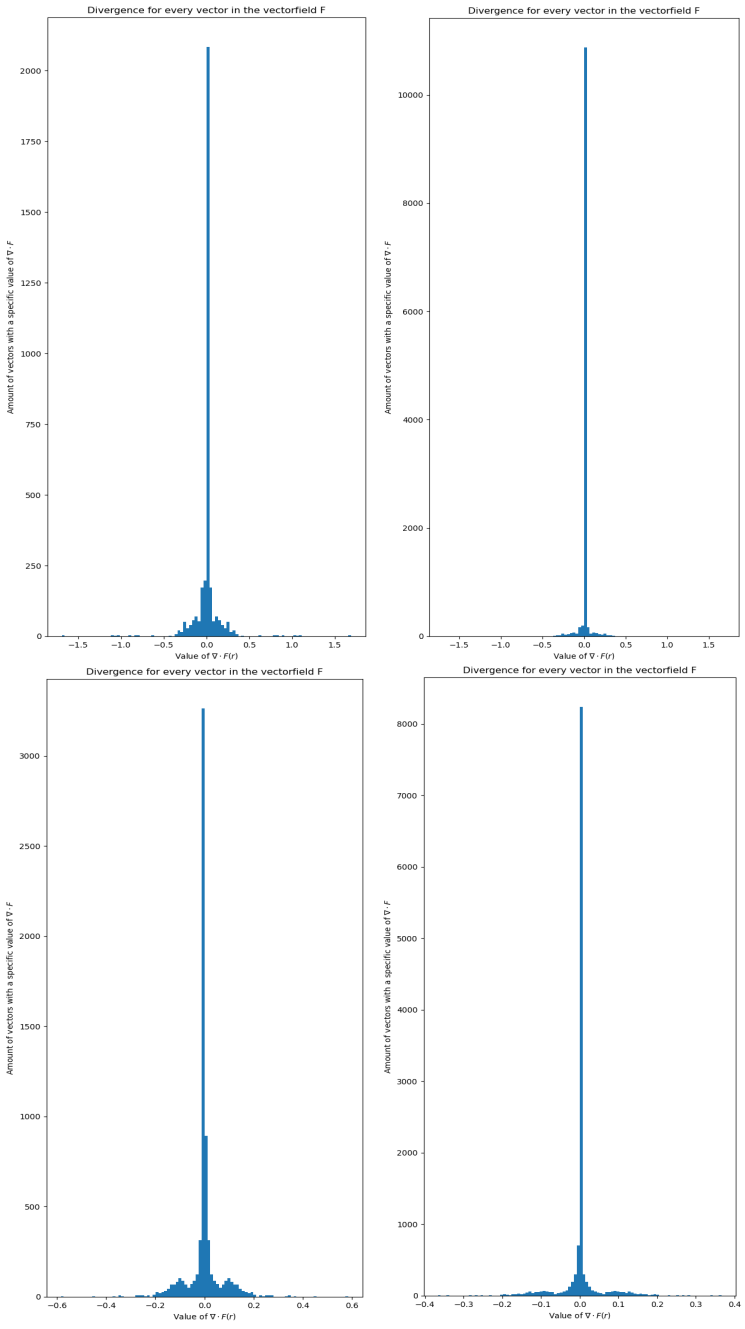

Figure 6: Divergence of every vector in the vector field **A** for different situations. Upper left: situation 2, lattice size 15x15x15. Upper right: situation 2, lattice size 23x23x23. Lower left: situation 3, lattice size 19x19x19. Lower Right: situation 3, lattice size 23x23x23

4.2 Simulation

Unfortunately, due to the fact that there were some issue's with the calculation of the Hopf index and the simulations themselves, they were unable to be performed. But the programming has resulted in a piece of code that can visualise the way the magnetisation vectors move during the energy minimisation.

5 Conclusion

Due to the fact that a number of troubling issues came to the surface during the later portion of the research the simulations failed to be performed in any meaningful way and thus no conclusion can be made from them. But the coding has resulted in a way to calculate the Hopf index of a vector field of a discrete simple cubic lattice to some accuracy. This calculation, as mentioned above, is correct for a specific set of conditions but will fail if they are not met.

6 Discussion

6.1 Improvements to Hopf index calculation

The main issue with the calculation of the Hopf index is that the value can't be used to check if a hopfion has appeared in a vector field. Even though the Hopf index is constant when the hopfion is far away from the boundaries of the system, it isn't constant when the hopfion sits close to the systems boundary, which it should be. Additionally this calculation could not be tested on hopfions with a Hopf index>1 as such hopfions would have multiple internal windings which would make it necessary to increase the hopfions size, else the hopfion can't be considered a smooth structure. Unfortunately, these larger hopfions wouldn't be able to fit in the maximum lattice sizes used in this research. To improve this, the Hopf index has to probably be calculated in a different manner; one way to do this is by radial basis function interpolation. With this method the vector field $\mathbf{F}$ is approximated:

$$\mathbf{F}(\mathbf{r}) = \sum_i (\nabla\nabla^T - \nabla^2)\mathbf{G}(|\mathbf{x} - \mathbf{x}_i|)\mathbf{c}_i \tag{29}$$

were $\mathbf{G}$ is the radial basis function and $\mathbf{c}_i$ are coefficients. An additional benefit of this calculation is that formula 29 automatically ensures that the vector field $\mathbf{F}$ is divergence free [17]. Using the coefficients obtained from formula 29 and the Coulomb gauge it is then possible to calculate the vector field $\mathbf{A}$ with the following formula:

$$\mathbf{A}(\mathbf{r}) = -\sum_i (\mathbf{c}_i \times \nabla)\mathbf{G}(|\mathbf{x} - \mathbf{x}_i|) \tag{30}$$

and thus the Hopf index can be calculated by performing numerical integration. The issue with radial basis function interpolation is that it is very computationally intensive and thus it may be necessary to make the appropriate approximations for larger systems.

6.2 Lattice

In this thesis all calculations have been performed on a simple cubic lattice but, in further research this should be expanded to include other lattice types. Changing the lattice type will consequently change some of the calculations which should thus be correctly adapted for the new lattice type.
It would also be of interest to look into ways to increase the lattice size used in the simulation in followup research. This will make it possible to search for not only larger hopfions, but also hopfions with a Hopf index greater than one. To make simulations with larger lattices possible on a reasonable time span some approximations have to be made which improv the simulation time.

6.3 Energy model

The Python library used in the simulation didn't give complete freedom in setting the energy function for the system. Unfortunately, complete freedom in

the energy function is quite desirable in the search for new models which could house hopfions and thus in further research it is important that this freedom will be acquired. The easiest way to do this is by looking for another simulation program which does give this freedom and using that for the simulations. The other solution is to write a new simulation program which lets you change the energy as you will; an added bonus is that you could implement the approximations used for increasing the simulation time for large lattice in the code as well.

7 bibliography

References

[1] Müller, G. P., Hoffmann, M., Dißelkamp, C., Schürhoff, D., Mavros, S., Sallermann, M., ... Blügel, S. (2019). Spirit: Multifunctional framework for atomistic spin simulations. *Physical Review B*, *99*(22), 224414.

[2] L. D. Faddeev, Lett. Math. Phys. 1, 289 (1976)

[3] T.H.R. Skyrme, Proc. Roy. Soc. 260, 127 (1961).

[4] Derrick, G. H. Comments on Nonlinear Wave Equations as Models for Elementary Particles. Journal of Mathematical Physics 5, 1252-1254, doi:10.1063/1.1704233 (1964).

[5] A. Bogdanov "New localized solutions of the nonlinear field equations", JETP Lett. 62, 247 (1995)

[6] Rybakov, Filipp Kiselev, Nikolai Borisov, A. Döring, L. Melcher, C. Blügel, Stefan. (2019), Magnetic hopfions in solids. digital image, accessed 17 may 2021 <https://www.researchgate.net/figure/Typical-structures-of-hopfions-a-Toroidal-hopfion-with-Hopf-index-H-1-The-solidfig1332140568>

[7] Rybakov, Filipp Kiselev, Nikolai Borisov, A. Döring, L. Melcher, C. Blügel, Stefan. (2019). Magnetic hopfions in solids.

[8] Tai, J.-S. B., Ackerman, P. J. Smalyukh, I. I. Topological transformations of Hopf solitons in chiral ferromagnets and liquid crystals. Proceedings of the National Academy of Sciences 115, 921, doi:10.1073/pnas.1716887115 (2018)

[9] Bernd Zimmermann. (2010), Dzyaloshinskii-Moriya Interaction in ultrathin magnetic Films: Cr/W(110). digital image, accessed 26 may 2021 <https://www.fz-juelich.de/SharedDocs/Downloads/PGI/PGI-1/EN/Zimmermann.diplompdf.pdf?blob=publicationFile>

[10] Moriya T. (October 1 1960). Anisotropic Superexchange Interaction andWeak Ferromagnetism. *Physical review*, *120*(1), 91.

[11] Gautam e, CC BY-SA 3.0 <https://creativecommons.org/licenses/by-sa/3.0>, via Wikimedia Commons

[12] Hopf, H. (1964). Über die Abbildungen der dreidimensionalen Sphäre auf die Kugelfläche. In *Selecta Heinz Hopf* (pp. 38-63). Springer, Berlin, Heidelberg.

[13] Whitehead, J. H. C. (1947). An expression of Hopf's invariant as an integral. *Proceedings of the National Academy of Sciences of the United States of America*, *33*(5), 117.

[14] A. A. Thiele, Phys. Rev. Lett. 30, 230 (1973).

[15] P. F. Bessarab et al. *Comp. Phys. Comm.* **196**, 335 (2015).

[16] N. Nagaosa and Y. Tokura, Nat. Nanotech. 8, 899 (2013).

[17] C. P. McNally, Mon. Not. R. Astron. Soc. 413, L76 (2011).